HANDLING CHARACTERISTICS CORRELATION OF A FORMULA SAE VEHICLE MODEL

Jason Ye
Team: Christopher Fowler, Peter Karkos, Tristan MacKethan, Hubbard Velie
Instructors: Jesse Austin-Breneman, A. Harvey Bell
Dept. of Mechanical Engineering, University of Michigan, Ann Arbor, Michigan
April 18, 2016

Abstract
Within the Formula SAE (FSAE) collegiate racing competition, quantitative and systematic decision-making strategies are crucial for the design and tuning of a competitive car. To provide direction for decisions, the MRacing FSAE team uses a model in VI-CarRealTime, a full-vehicle simulation environment. This project aimed to correlate handling-critical chassis parameters of this model to on- and off- vehicle test data. Specifically, values were determined for the Pacejka tire model coefficients and the model's aerodynamic downforce and drag. Baseline tire model coefficients were fitted to flat belt force and moment (F&M) data, and a baseline aerodynamic map was created from full-car wind tunnel testing results. The car was then simulated and physically tested through quasi-steady state and open-loop maneuvers. The longitudinal and lateral tire coefficients and the downforce and drag values were scaled to fit the simulation outputs to straight-line and increasing steer test data. The F&M measurements were found to overestimate tire forces, while wind tunnel measurements underestimated downforce and drag values.

Introduction
MRacing competes annually in Formula SAE, a collegiate competition series that tasks university teams to design, fabricate, test, and compete small, formula-style cars [1]. The dynamic events of the competition gauge the performance of the cars in straight-line acceleration, constant-radius cornering on a skid pad, and handling and reliability on an autocross track. The competition's rules are mainly safety-related, giving teams the freedom to control most of their vehicle design. As a result, the MRacing team makes decisions affecting vehicle handling every year throughout the design process and leading into competitions to improve its overall scoring.

To provide guidance for design decisions, the team utilizes a 14-degree-of-freedom ADAMS/Car derivative vehicle model in VI-CarRealTime. In the model, most vehicle subsystems are included as lookup tables with nonlinear spline interpolations. Although some of the parameters of the model for MRacing's 2015 car, MR-15, were directly measured from the car, many were estimates determined from computer-aided engineering tools or subsystem-level tests. In addition, a new model must be built every year for each new car that is built, and unknown parameters are sometimes ported from legacy models as best guesses. As a result, there were discrepancies between the simulation outputs and sensor measurements recorded in the vehicle,

as shown in Fig. 1 for an increasing steer event. These outputs and this event are discussed further in the Methodology.

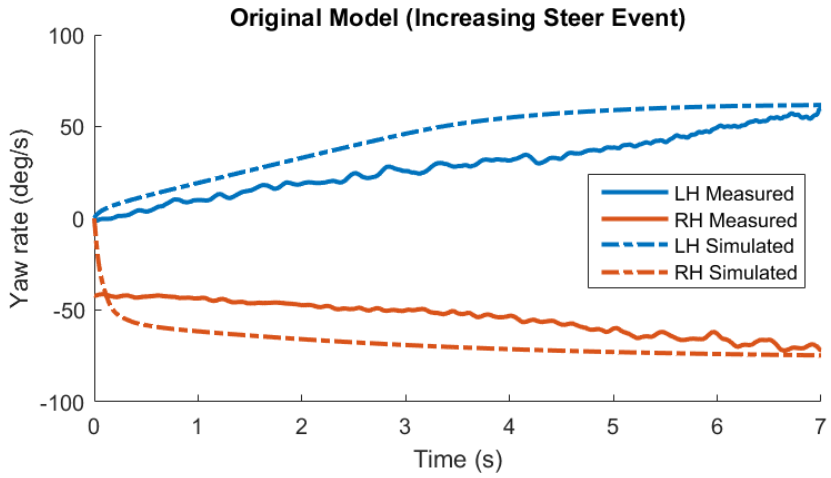

Figure 1. The yaw rate of the simulated model deviated significantly from that measured on the car in the increasing steer event. Both left-hand (LH) and right-hand (RH) turns are shown.

In the simulation, a driver model is used to control the car through course events. This project examines vehicle outputs in open loop and quasi-steady state events to eliminate effects from inaccuracies in the driver model and to provide a solid foundation for further model validation. Specifically, the events of focus were straight-line acceleration, coastdown, constant steer, and increasing steer, as is discussed in the Methodology. The tire model and aerodynamics map were selected as parameters of interest for their influence, as determined from prior experience, on handling performance due to their direct interactions with the environment. Because of the tire model's complexity and the aerodynamic map's prior basis on unvalidated predictions from computational fluid dynamics, the team also lacked confidence in these aspects of the model.

Tire Model

The tires (Hoosier LC0 6.0/18.0-10) are represented using the 2002 Pacejka "Magic Formula" model, first developed in the 1980s and still widely used in automotive simulation [2]. This model is considered semi-empirical, as it is based on measured data but contains a structure with some basis on physical relationships. Note that in this paper, discussion of tires uses the SAE tire axis system [3]: the *x*-axis is the direction of the wheel heading, and the *y*-axis points (in the road plane) to the right when viewed from above with the *x*-axis forward. This definition is shown in Fig. 2, p. 3.

In the model, the lateral force output by the tire, F_y, is a function of the slip angle, α, which is defined as the angle between the tire's heading direction and its velocity vector (see Fig. 2, p. 3). The longitudinal force, F_x, in the model is a function of the slip ratio, κ, defined as follows:

$$\kappa = \frac{\text{driven/braked wheel angular velocity}}{\text{free-rolling wheel angular velocity}} - 1 \qquad \text{(Eq. 1)}$$

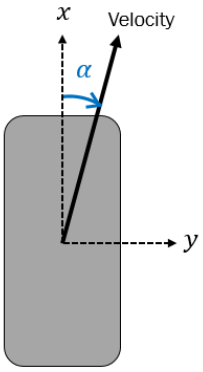

Figure 2. The SAE tire axis system, top view

The general form for F_x and F_y at one set of conditions is given by Pacejka [4] as:

$$F = D\sin[C\arctan\{Bk - E(Bk - \arctan Bk)\}] \qquad \text{(Eq. 2)}$$

where F in the equation is either F_y (with $k = \tan\alpha$) or F_x (with $k = \kappa$). B is the stiffness factor, C is the shape factor, D is the peak value, and E is a curvature factor, which are functions of normal load and camber angle. Shift factors can be added to F and/or k to generate offsets from the origin and "user scaling factors" λ can be applied to all of these factors, as well as other intermediate factors not discussed, to adjust for friction characteristics of a road surface different than that tested.

Aerodynamic Map

The aerodynamic properties of the vehicle model are stored in a lookup table that gives the downforce (lift acting towards the ground) and drag experienced by the vehicle, with the front ride height and the rear ride height as independent variables. The drag is applied at a single point of the car, while the downforce is applied at two points, one at the front and the other at the rear, as shown in Fig. 3.

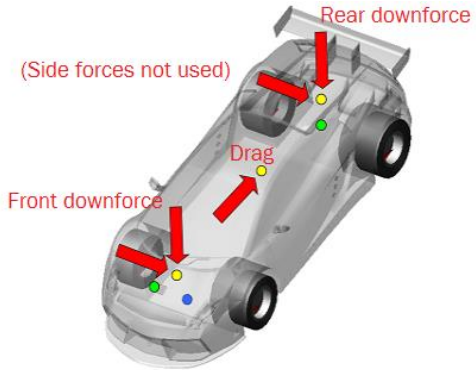

Figure 3. Downforce and drag application points, as shown in the VI-CarRealTime program

Methodology

Track Test Events

MR-15 was tested in the following events in July 2015 at the Fowlerville Proving Ground, provided by FT Techno of America. The vehicle had a host of sensors installed, including an accelerometer, a yaw rate sensor, wheel speed sensors, a steering potentiometer, damper potentiometers, a throttle position sensor, a brake pressure sensor, and a tachometer. Accelerometer measurements were sampled at ~200 Hz, while most other readings were sampled at 100 Hz.

Straight-line Acceleration: From a stopped position, full throttle was applied. The driver shifted gears between 11,000 and 11,500 RPM, and the car was allowed to reach its top speed of approximately 122 kph (33.9 m/s).

Coastdown: The car was accelerated to a speed of 100 kph (27.8 m/s), shifted into neutral, then allowed to coast until it no longer had room on the track, which occurred at a speed of approximately 45 kph (12.5 m/s)

Constant Steer: The car was turned at a constant steer angle and constant speed of approximately 45 kph (12.5 m/s) for 5 sec. This was performed for turns in both directions at steering wheel angles under 55°.

Increasing Steer: The car was brought to a speed of 40 kph (11.1 m/s), and the driver increased the steering wheel angle at a constant rate of approximately 4 °/s from straight-ahead until maximum steer while maintaining said vehicle speed. This was performed in both directions.

Tire Model

Baseline Coefficients: To determine baseline coefficients for the tire model in longitudinal and lateral slip, force and moment (F&M) test data was fit to the Pacejka equation form. The F&M testing was performed in February 2012 by the Formula SAE Tire Test Consortium, an organization of member universities that pool their resources to perform tire testing at the Calspan Tire Research Facility. The tire was mounted on a machine that controlled its orientation and measured forces and moments at the spindle, while the tire was run over a flat belt with a friction surface similar to sandpaper, as shown in Fig. 4, p. 5.

A cornering test and a drive/brake/combined test were performed at 40 kph (25 mph) at pressures between 55 kPa (8 psi) and 97 kPa (14 psi), at inclination angles between 0° and -4°, and at normal loads between -222 N (-50 lbf) and -1560 N (-350 lbf). In both tests, the tire was initially put through a warm-up period of about 1 min. For the cornering test, it was repeatedly swept through α values of ±12° at 4°/sec for each combination of conditions, and for the drive/brake/combined test, the tire was "swept" through κ values of ±20% at three slip angles, 0°, -3°, and -6°.

Figure 4. F&M testing at the Calspan Tire Research Facility. Photo from FSAE TTC.

OptimumTire, a dedicated tire analysis software tool, was used to perform the coefficient fitting for this data. The inflation pressure of 55 kPa was used, as this was approximately the value of tire pressure run in the vehicle tests. The measured data values were separated into clusters dividing discrete test conditions in order to remove hysteresis effects and hasten the fitting process. Using an iterative least squares algorithm, the F_y and F_x coefficients were determined separately.

Coefficient Scaling: The coefficients dictating F_x were scaled to match simulation outputs from the acceleration event to measured data. First, the accelerometer data from the coastdown tests was used find F_{losses}, the combined losses (as a force) from drag, rolling resistance, and friction as a function of V_x, the longitudinal velocity according to the following relationship:

$$m_{total}A_{x_{meas}} = F_{drive} - F_{brake} - F_{losses} \qquad \text{(Eq. 3)}$$

where m_{total} is the total vehicle mass, $A_{x_{meas}}$ is the measured longitudinal acceleration, and F_{drive} and F_{brake} are the total drive and brake forces, respectively. F_{drive} and F_{brake} were taken to be negligible in the coastdown test.

The quadratic fit of F_{losses} was then applied to the measured car forces in the acceleration tests to calculate F_x, the longitudinal force output by the rear tires, assuming equal contributions from both sides of the car. Also, κ was calculated using the wheel speed sensor readings at the front as the free-rolling wheel velocity and those at the rear as the driven wheel velocity in Eq. 1, p. 2. This enabled the creation of F_x vs. κ plots from the test.

Each acceleration event was also simulated in CarRealTime, with the speed range of each gear as a separate event. The longitudinal coefficient scaling factors were adjusted manually to minimize the error between the simulated F_x vs. κ relationship and that obtained from measurements.

The F_y coefficient scaling factors were adjusted to match the simulation output yaw rate plot over time with that obtained from the increasing steer test. The simulated test used a linear fit of the steering potentiometer values throughout the test. To verify the steering potentiometer readings, the lateral acceleration, a_y, was compared between the constant radius tests and simulated constant radius events at the measured steer angles.

Aerodynamic Map

Baseline Map: MR-15 was tested at a wind tunnel run by Fiat Chrysler Automobiles. Various configurations of the aerodynamics package at different pitch and yaw angles of the car were tested at 48-97 kph (13-27 m/s) while the forces at each tire were measured.

Using 64 kph (18 m/s) as the reference velocity, measured downforce and drag values for each tested pitch angle were entered into the map at the corresponding ride heights. Intermediate values were linearly interpolated.

Force Scaling: Scaling factors for the front downforce in the model were applied to fit the baseline map from simulated acceleration events to the track data. To find the front downforce in the physical tests, calculations were performed on damper potentiometer readings by approximating each corner of the vehicle as the mass-spring-damper system shown in Fig. 5 [6], where k_u is the effective spring rate of the wheel, k_s is the rate of the ride spring, and c_s is the damping constant of the parallel damper. Because of the quasi steady state assumption, damping was ignored—the force acting on a corner of the car (from equilibrium) is equivalent to $k_s(x_s - x_u)$, where $(x_s - x_u)$ is the measured spring/damper displacement from its equilibrium position.

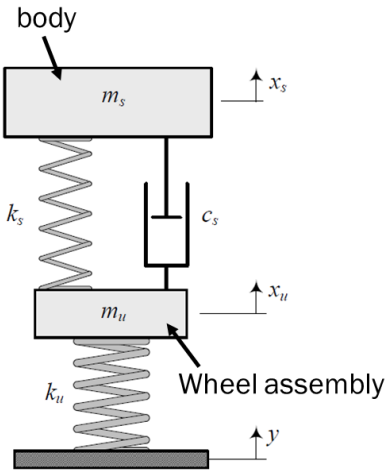

Figure 5. Mass-spring-damper approximation for corner of vehicle [6]

The rear damper potentiometer outputs were too noisy to be usable, even after filtering. This was likely due to engine vibrations and wear on the potentiometers. As such, the front downforce scaling factor was applied to the rear. This scaling factor was also applied to the drag force, as other methods could not be used with the available data without introducing excessive error.

Results

Tire Model

Baseline coefficients: The baseline lateral (F_y) Pacejka model coefficients were fit with 4.7% error and the longitudinal coefficients were fit with 6.3% error, as shown in Fig. 6 for a representative inclination angle and normal load pair (2° and -1015 N).

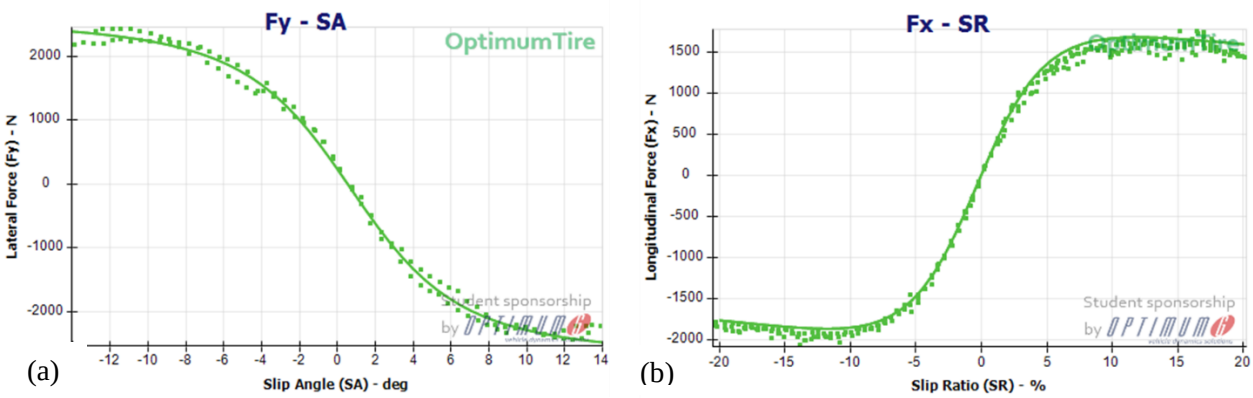

Figure 6. Baseline Pacejka model fits, where points are measured data and the curve is the fit. Note that SA in the figure is α and SR in the figure is κ.

Generally, the fit for each condition is better at low slip angles and low slip ratios, in the linear range of the tire. The F&M data showed F_y to decrease from intermediate to high slip angles (8° to 14°), while the model predicted the force to remain relatively constant. The fit for F_x was significantly better for positive κ (acceleration) than for negative κ (braking). Although the Pacejka model has terms to account for this asymmetry, the least-squares fit did not produce coefficients to sufficiently address the observed effect.

Coefficient Scaling: The scaling of longitudinal coefficients gave acceleration event outputs with a standard error of 141 N, as shown in red in Fig. 7 with the test track calculations shown in blue.

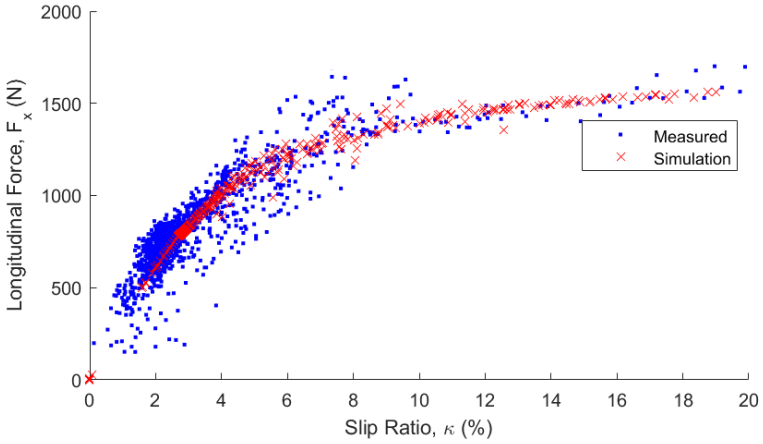

Figure 7. Simulation outputs of the scaled longitudinal tire model (red) plotted with measured data (blue)

There was a significant amount of noise from the sensor data that could not be filtered out for low to intermediate κ, mainly as a result of noise in the accelerometer readings. Although the fit appears to be good for high slip ratios, there were fewer data points in that region because the initial launch of the vehicle was not included in this data. Note that the tire model is unable to represent a stationary state, so the simulation was started at a non-zero initial velocity.

The scaling of the lateral coefficients resulted in a standard error of 6.8 °/s in the yaw rate response of the simulated left-hand and right-hand increasing steer event, as shown in Fig. 8. Almost half of the event was truncated due to slight variations in the driver's steering wheel rate, which is the source of the offset starting point for the right-hand increasing steer. The simulation had difficulty matching both the low- and high-steer angle responses, so a compromise was used for the coefficient fit.

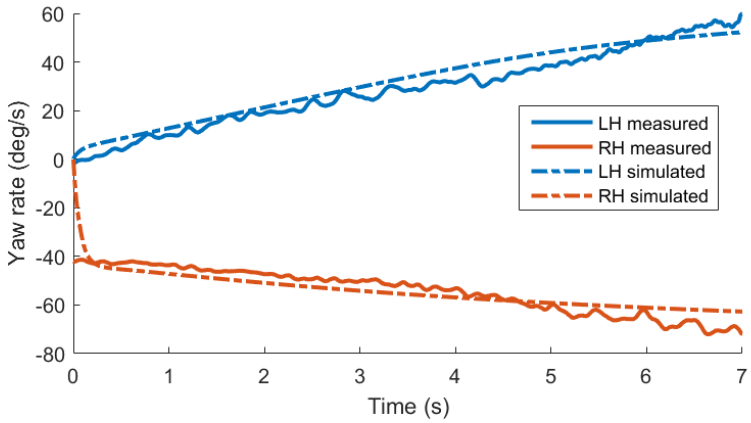

Figure 8. Yaw rate in the increasing steer event. The solid line represents the measured rate, while the dashed line is the simulation predicted yaw rate.

Aerodynamic Map

The baseline map was created directly from wind tunnel measurements, so it is not included.

Force Scaling: A 1.2 scaling factor was applied to the front downforce to produce the output from the acceleration event shown in Fig. 9, with a standard error of 59.4 N.

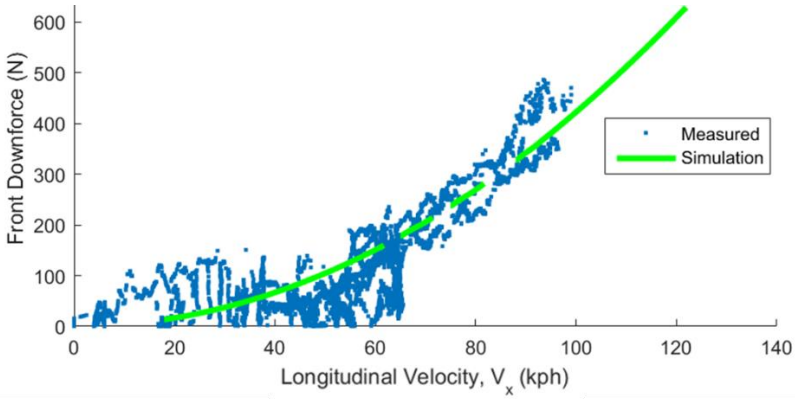

Figure 9. Front downforce from simulation and from vehicle measurements

The gaps in the simulation downforce curve are at the car's gear changes. There was still significant noise remaining after filtering the measured downforce, resulting from the use of damper potentiometers to calculate those values. Due to this, the downforce at low velocities was mostly ignored during the fitting process.

The longitudinal acceleration from the similarly-scaled drag force in the simulation was compared to accelerometer data in the coastdown event, as shown in Fig. 10. Error calculations were not performed, as the simulation outputs are not expected to fit the data—rather, this comparison was performed for reference. The measured coastdown acceleration, as discussed in the Methodology, is a result of not only aerodynamic drag, but also rolling resistance and friction from joints and bearings. Thus, the simulated drag should under-predict the acceleration, as is evident at lower velocities. The plot shows that aerodynamic drag dominates at higher velocities, suggesting that it increases at a faster-than-linear rate with speed (possibly quadratic, depending on the characteristics of the flow around the vehicle).

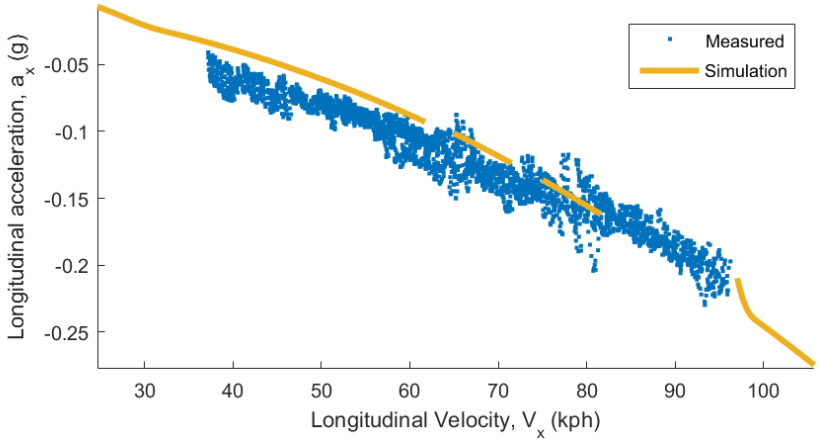

Figure 10. Acceleration from drag output by the simulation, overlaid with the measured acceleration in the coastdown tests

Conclusions

In this project, the tire model and aerodynamic description of the MR-15 vehicle model were correlated to open loop and quasi-steady state tests. Scaling factors were applied to baseline Pacejka coefficients from force and moment tire test data fitting, as well as to a baseline aerodynamic map created from wind tunnel test data. For these fits, error values in the range of 7-12% were achieved despite noise in sensor readings.

Because some of the metrics used in this project to gauge vehicle handling were the result of calculations performed on sensor measurements, they were very sensitive to measurement variations caused by inaccuracy or noise. For this reason, it is critical that all vehicle sensors are calibrated and tested, ideally on their own, before use. Additionally, it was found that even in the standard testing performed for this project, it was difficult to completely isolate the driver—any future closed loop correlation would need to comprehensively address this issue.

This work was performed on a previous year's car, but some of the results, like the tire model, can be directly utilized in a current model. However, care should be taken to characterize differences in the conditions under which the previous tests were performed and those that would prevail in future tests, especially road surface variations and temperature/pressure effects. The author hopes that this project will serve as a starting point for future work in the team to better understand the race car and to better utilize its simulation tools.

References

[1] SAE International, 2016, "2016 Formula SAE Rules," from http://www.fsaeonline.com/content/2016_FSAE_Rules.pdf.

[2] Cabrera, J. A., Ortiz, A., Carabias, E., and Simon, A., 2004, "An Alternative Method to Determine the Magic Tyre Model Parameters Using Genetic Algorithms," Vehicle System Dynamics, **41**(2), pp. 109-127.

[3] Society of Automotive Engineers, Inc, 1970, "Vehicle Dynamics Terminology," SAE J670e.

[4] Pacejka, H. B., 2002, *Tyre and Vehicle Dynamics*, Butterworth-Heinemann, Oxford, U.K.

[5] Jazar, R. N., 2008, *Vehicle Dynamics: Theory and Application*, Springer, New York, NY, Chap. 15.